Available online at www.sciencedirect.com

ScienceDirect

Procedia CIRP 71 (2018) 348–353

www.elsevier.com/locate/procedia

4th CIRP Conference on Surface Integrity (CSI 2018)

Residual Stress in Metal Additive Manufacturing

C. Li[a], Z.Y. Liu[a], X.Y. Fang[b], Y.B. Guo[a,*]

[a] *Dept. of Mechanical Engineering, The University of Alabama, Tuscaloosa, AL 35487, USA*
[b] *Institute for Advanced Manufacturing, Shandong University of Technology, Zibo 255049, China*

* Corresponding author. Tel.: 1-205-348-2615; fax: +1-205-348-6419. *E-mail address:* yguo@eng.ua.edu

Abstract

Additive manufacturing (AM) has been widely used to fabricate functional metal parts in automobile, aerospace, energy, and medical device industries due to its flexible process capacity including complex geometry, functional graded materials, and free usage of tool. For the two major categories of metal additive manufacturing processes include powder bed fusion (PBF) and directed energy deposition (DED), parts are fabricated through melting of feed stock materials in the form of either powders or wires directly from a CAD model. The unique thermal cycle of metal additive manufacturing is characterized by: (1) rapid heating rate due to high energy intensity with steep temperature gradients; (2) rapid solidification with high cooling rates due to the small volume of melt pool; and (3) melt-back involving simultaneous melting of the top powder layer and re-melting of underlying previously solidified layers. Residual stress caused by the unique thermal cycle in AM is the critical issue for the fabricated metal parts since the steep residual stress gradients generate part distortion which dramatically deteriorate functionality of the end-use parts. This paper comprehensively assessed the current research status on residual stress sources, characteristics, and mitigation. First, the relationship between residual stress and microstructure is highlighted in AM metal parts. Then, the measurement methods and characteristics of residual stress in both as-build metal parts and post-processed ones were summarized. Third, residual stress mitigation and control methods including in-situ and post-process control methods were thoroughly discussed. Furthermore, future work directions are provided in this work.

Selection and peer-review under responsibility of the scientific committee of the 4th CIRP Conference on Surface Integrity (CSI 2018).

Keywords: Surface integrity; residual stress; additive manufacturing

1. Introduction

Additive manufacturing (AM) has been widely used to fabricate functional metal parts in a variety of industries due to its flexible process capability [1,2]. Most of the metal AM technologies enable complex geometry and functional part fabrication by gradually adding thin layers of metals based on a digital model without need for tooling and assembly when compared to conventional manufacturing processes [2,3].

There are two major types of metal AM process depending on the fashion of material deposition: powder bed fusion (PBF) and directed energy deposition (sheet lamination is not included in this study). In PBF, high energy beam, either laser beam or electron beam is used to fully melt thin layers of metal powders in an inert or vacuum atmosphere out of a powder bed to produce a 3D object. In a typical laser based PBF setup (selective laser melting SLM) [4], single or multiple laser sources are used to fully melt 30 - 50 µm thick powder layers in an inert atmosphere. Electron beam melting (EBM), first commercialized by Arcam, is another type of PBF process which uses electron beam as heat source to melt metal powder materials in a high vacuum chamber with a layer thickness (100 µm) typically higher than laser PBF process [5]. A key characteristic for EBM is that a significate powder bed preheating is applied to reduce temperature gradient and residual stress of the build when compared to SLM [6]. Unlike PBF, DED produces parts by directly melting feed stock material either through feeding powder or feeding wire. Like PBF, heat source in DED is usually laser or electron beam. However, DED has much higher material deposition rate compared to PBF [7,8], because of the thicker layer thickness and higher energy deposition rate. But the downside for DED is that it holds lower part accuracy than PBF. Beside higher deposition rate, other advantages of DED

Selection and peer-review under responsibility of the scientific committee of the 4th CIRP Conference on Surface Integrity (CSI 2018).
10.1016/j.procir.2018.05.039

over PBF are that DED is more feasible to manufacture small features on curved surface and to remanufacture high value components when coupled with machining process [8]. Other metal AM processes like binder jetting or metal FDM (fused deposition modeling) utilize a binder agent to first form a green part and then sintered to obtain a near full dense part [9].

The unique thermal cycle of metal AM is characterized by the rapid heating, cooling rates, and melt-back involving simultaneous melting of the top material layer and re-melting of underlying previously solidified layers. Residual stress caused by this unique thermal cycle in metal AM is a critical issue for the manufactured parts since the steep residual stress gradients would generate part distortion [10,11]. A during-process part distortion may result in recoater blade damage in the case of PBF, distortion of the final part would dramatically deteriorate its functionality. Several methods have been studied to reduce residual stress and part distortion in metal AM [10,12]. Decreasing temperature gradient through preheating the feed stock material or the substrate is the most used approach to reduce residual stress [12-15]. Numerous published or ongoing works have been focusing on wide variety issues of metal AM process: from processability, metrology, surface integrity, to functionality. This study is focused on the residual stress issue in PBF and DED process.

2. Residual stress sources in metal AM

2.1. Residual stress formation model

As mentioned in the previous section that the unique rapid heating-cooling thermal cycle of AM, which is very similar to welding process, leads to residual stress in AM part. To certain extent, welding and AM share similar residual stress formation mechanism [16]. Temperature gradient mechanism (TGM) model and cool-down phase model have been mentioned by Mercelis et al. [11] to explain the residual stress formation mechanism. In TGM model, during heating state, the heat source with high energy intensity heats up the feed stock material rapidly and the heated material tends to expand but this thermal expansion is restrained by the surrounding materials with lower temperature. Thus, a compressive stress state is formed located at the heated zone. During the cooling stage when the heat source is removed, the previously formed heated zone begins to cool down and a shrinkage of materials in this zone tend to occur, but the shrinkage is partially restrained by the plastic strain formed during the heating stage. Finally, tensile residual stress is formed in the heated zone which is balanced by a compressive zone. The cool-down phase model is another explanation for residual stress formation mechanism for metal AM due to its layer build-up process characteristic [11]. Most of the previously melted material will experience a remelting and re-solidification cycle. The cooling down cycle after re-solidification of the material also leads to material shrinkage which is fractionally restrained by the previously deposited material and a tensile stress state is formed in the newly deposited material. Although the narrative description is helpful to understand residual stress, but the graphic model do not match the contents. Therefore a new model of residual stress formation is proposed in Fig. 1. In a practical AM process, the residual stress field is much more complicated since the number and pattern of heat source path and heat transfer are extremely complex.

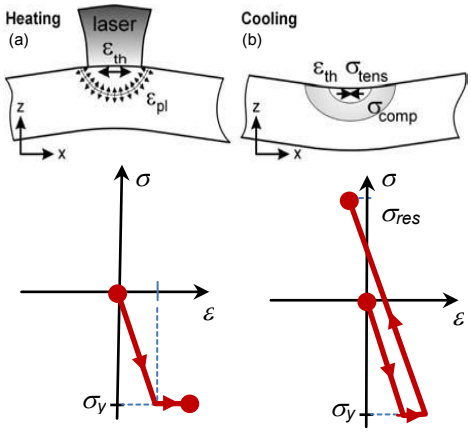

Fig. 1. Residual stress formation model: (a) heating-phase, (b) cooling-phase

2.2. Residual stress types and measurement techniques

Residual stresses could be categorized by different length scale: type I, type II, and type III [17]. Type I residual stress is on macrolevel. Type II stresses or microscale stress nearly always exist due to anisotropic material properties on grain scale, and type III stress is on nanoscale and is due to coherency and dislocation [17]. Type II and type III residual stresses have very limited effect on the material's mechanical properties and beyond the scope of most of the current measuring methods [11]. However, very localized microscale or nanoscale residual stress could be measurable using focused iron beam milling with digital image correlation [18] or nanoindentation along with transmission electron microscopy (TEM) [19].

Some studies have indicated that a post heat treatment of the as-build AM part would dramatically reduce the dislocation density through TEM observation, which provides a qualitative estimation of significant reduction of residual stress type III [20,21]. If not specified, the residual stress discussed in this paper would be type I stress since its macroscale characteristics would affect the surface integrity of AM metal parts. Table 1 summarizes the major residual stress measurement methods in metal AM. The most widely applied nondestructive method in AM is X-ray and neutron diffraction method which could provide near-surface and volumetric stress field [22].

Table 1 Residual stress measurement techniques in metal AM [17,22]

Method	Penetration	Resolution	Accuracy	Cost
Hole drilling	Size of hole dia.	50-100 µm depth	± 50 MPa	Low
Curvature	0.1-0.5 of thickness	-	Minimum measurable	Medium
X-ray diffraction	Near-surface	1 mm lateral, 20 µm depth	± 20 MPa	High
Neutron diffraction	volumetric	500 µm	± 40 × 10^{-6} strain	High

2.3. Residual stress and microstructure

Metal AM is a highly non-equilibrium process and usually results in heterogeneous microstructure where lattice spacing

is highly location dependent. Typical materials such as nickel based superalloys, titanium alloys, and stainless steels applicable in metal AM show columnar microstructures and strong texture in build direction [23-25]. Residual stress components in different directions and in different location could be quite different due to the location dependent lattice spacing resulted from AM. When applying diffraction measurement such as X-ray or neutron on an AM part, a location-dependent reference lattice spacing must be used [26]. Wang et al. [26] utilized stress-free lattice spacing determined from stress relief treated DED samples and the neutron diffraction measured residual stress field obtained very good agreement with numerical prediction.

3. Residual stress characteristics in metal AM

Residual stress field of metal AM parts could depend on scanning strategies, dwell time and many other process parameters that have huge impact on thermal history. Wu et *al.* [22] studied the surface-level residual stress of SLM processed stainless steel 316 L-shaped bar (off substrate) in as-build state by digital image correlation method and neutron diffraction. Residual stress near the center of part tends to be compressive and tensile near surfaces as shown in Fig. 2a. Effects of parameters including scanning strategy, laser power, scanning speed, and build orientation on residual stress has been systematically investigated. A smaller scan island size and increased length energy density would result in a reduced residual stress field. Kruth *et al.* [27] studied the effects of scanning strategies on distortion and concluded that the island scanning strategy (material deposited in a "chessboard" pattern) would cause less distortion than other scanning strategy. Lu et al. [28] also explored the effect of island size on residual stress and similar trend was observed compared to [22]. It was found that the island size of 2×2 mm^2 resulted the smallest residual stress, but severe cracking was also observed in the sample built using this island size. An island size of 5×5 mm^2 was considered the optimal strategy due to higher density, better mechanical properties, and relatively lower residual stresses. Mercelis et al. [11] also concluded that high tensile residual stress in build direction of a cutoff part in as-build state is located just below the top surface followed by a compressive zone in the middle and a tensile zone at the bottom surface. And this trend was also captured by simulation work [29] as shown in Fig. 2b that a large compressive residual stress was predicted in the core of the part and experiment work of DED processed Waspaloy by Moat et al. [30].

X-ray diffraction residual stress measurement of SLM processed stainless steel and Ti6Al4V small-sized samples conducted by Yadroitsev et al. [31] has shown that residual stress in scanning direction is more tensile than in the perpendicular direction and reaches its maximum at the build-substrate interface. Kruth *et al.* [15] assessed the residual stress of the SLM processed part using the bridge curvature method. The method has also been adapted by other researchers [32,33] to fast evaluate residual stress of SLM processed part. The level of residual stress of the bridge-shaped part is characterized by the curling angle of the two bottom surfaces of the bridge after it is removed from the substrate. Process parameters including scan vectors length and rotation angle of scan vectors for two sequential layers were considered and it suggests that a shorter length of scan vectors and larger rotation angle are preferred for limiting residual stress and deformation during the SLM process.

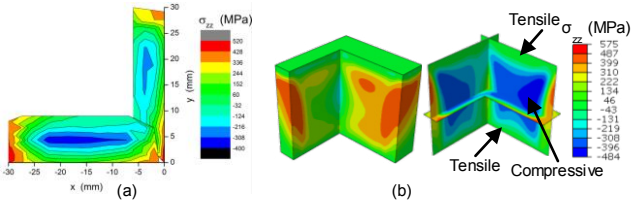

Fig. 2. Typical residual stress in build direction of as-SLM part w.o. the substrate: (a) cross-sectional residual stress contours measured using neutron diffraction [22], (b) predicted residual stress [29].

Compared to SLM, EBM processed part has much lower level of residual stress due to approximately an order of magnitude lower of cooling rate judging by the resulted solidification features such as dendrite arm spacing of these tow processes [23,34,35]. The much lower cooling rate in EBM is caused by the significant preheating of powder bed and isolated vacuum chamber, and it takes longer for the heat to dissipate from the EBM part. Sochalski-Kolbus et al. [36] experimentally compared the residual stress distribution of Inconel 718 cubes processed by EBM and SLM in as-build state using neutron diffraction. Electrical discharge machining (EDM) was used to prepare stress-free sample for determining stress-free lattice spacing. They found that each residual stress component resulted by EBM is an order magnitude lower by SLM since SLM is further from equilibrium state than EBM.

For similar reason as SLM, significant residual stresses could also develop in the part processed by DED process. De Oliveira et al. [37] characterized residual stresses in Co-based laser deposited claddings using X-ray diffraction. The stress state of the Stellite 20 coating near the surface is biaxial tension, but the major component is much larger than the minor one. Rangaswamy et al. [38] investigated the residual stress of SS 316L and Inconel 718 parts fabricated by DED using neutron diffraction and contour method. The residual stress at the center of the samples was uniaxial compression. Tensile residual stresses were observed at the edges and aligned along the build direction. And the magnitudes of the residual stresses exceeded 50% to 60% of the nominal yield strength of the material. Denlinger et al. [39] investigated the effects of dwell time on the residual stress and distortion of DED processed Ti64 and Inconel 625 build. These two materials exhibit exact opposite trend, where increasing of cooling time during the deposition process would generate lower residual stress for Inconel 625 build. On the other hand, reducing the cooling time for Ti64 build would resulted in much lower level of residual stress which is caused by a stress relaxation due to solid phase transformation when a certain temperature level was reached during the DED process [40]. Szost et al. [41] studied the residual stress of Ti64 thin wall build prepared by wire-arc based DED and laser DED process. The maximum residual stresses were located at the build-substrate interface for both builds and wire-arc process tends

to generate higher residual stress level compared to laser DED process since wire-arc has much higher heat input than laser. In addition, the substrate removal in as-build state would significantly reduce the residual stress levels but generate additional part distortion. This phenomenon has been captured by many experimental [12,15,32,33,42] and numerical studies [43-46]. A build-on-plate stress relief heat treatment would be very necessary for limiting part distortion in laser PBF and DED process.

4. Residual stress mitigation and control

4.1. In-situ process control

In-situ control methods for reducing residual stress could be categorized as: in-situ feedback control, thermal gradient control, scanning strategy control, and mechanical control. In-situ feedback control aims to change and homogenize the temperature distribution of the part during the process. Many ongoing research activities have been focusing on the in-situ thermal monitoring of PBF process using IR cameras to characterize melt pool, deposition, and powder bed temperature, to identify hot or lack of fusion spot during the process [47-50]. A relatively even distributed temperature field of the build surface, reduced thermal gradient, and reduced residual stress level is achievable through closed-loop feedback control in PBF. Closed-loop control has been well established in DED since it has been developed prior to PBF. However, closed-loop feedback control of parameters such as laser power, scan speed in real time would be difficult owing to poor spatial resolution, limited fields of view due to the harsh operation environment of PBF, and large load of data to be processed [51]. Most current applicable and effective method to in-situ reduce residual stress would be thermal gradient control which aims to reduce thermal regredient within the build during the process by preheating substrate [12,52,53] or powder bed [54-56]. Mechanical control method balances out the high tensile residual stress by introducing an in-situ compressive pressure, such as laser shock peening (LSP) [57-59] or rolling [60,61].

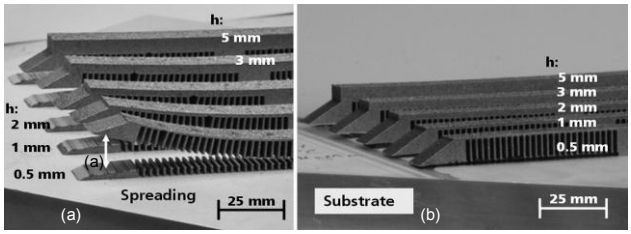

Fig. 3. Effects of preheating of substrate on cut-off distortion of AlSi10Mg build prepared by SLM: (a) no preheating, (b) preheated at 200 °C. [12]

Preheating of either substrate or powder bed has been widely used to reduce residual stress and produce crack-free components in SLM. Buchbinder *et al.* [12] systematically investigated the effects of substrate preheating temperatures on the distortion of AlSi10Mg twin cantilever by SLM. Like the bridge structure method, the support structure of cantilever was cut off and the spring back distance of the cantilever arms represents the magnitude of residual stress as shown in Fig. 3. Significant distortion reduction was observed when the substrate was preheated to 200 ℃ for the AlSi10Mg build as shown in Fig. 3b. Ali et al. [56] implemented a customized powder bed heater to a commercial SLM machine to study the effect of powder bed preheating temperature on residual stress. The maximum principal stress decreases as the powder bed preheating temperatures increases. Preheating temperature higher than 570 ℃ would result in zero residual stress or even compressive residual stress which would be beneficial for fatigue performance. Inhomogeneous microstructures would be generated due to different thermal gradient near the substrate compared to bulk [7]. Controlling of scanning strategy is also used to reduce residual stress [27]. Concept Laser has developed an innovative LaserCUSING® approach in which the laser scanning pattern is selective controlled through an algorithm to minimize residual stress. Applying a compressive mechanical load through laser shock peening or rolling on the part surface to cancel out or reduce the magnitude of the tensile residual stress is another group of method to in-situ control residual stress in metal AM. Hybrid AM process coupled with machining, laser shock peening, rolling etc. is described in reference [62]. Kalentics et al. [58] explored the capability of laser shock peening to tailoring residual stress in SLM and found that the surface tensile residual stress could be easily altered into beneficial compressive residual stress with a depth more than 1 mm when a high overlap ratio of laser spot was used (see Fig. 4). Limitations for in-situ control of residual stress using LSP could be that LSP facility is difficult to integrate with commercial SLM machines, and LSP might significantly expand the part printing time. Another method using mechanical load to control residual stress is in-situ rolling which could be potentially feasible for metal AM process with large material deposition rate such as wire-based DED or other wire-arc based AM processes [61].

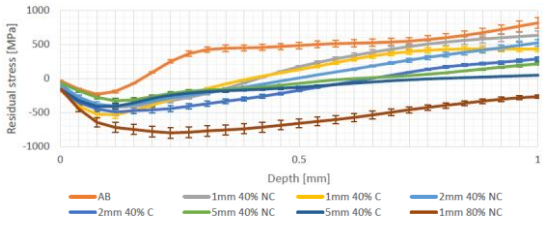

Fig. 4. Tailoring residual stress by laser shock peening [58].

4.2. Post-process control

Post heat treatment process is widely used to homogenize the microstructure and tailoring mechanical properties of as-build AM components and to increase the ductility at the expense of lowering tensile strength [63]. A post annealing of as-build AM part would reduce 70% of residual stress [10]. Machining as post-processing is widely used to improve surface finish of part after AM process. And it is well understood that machining processes like hard turning and grinding would generate compressive residual stress on the machined surface and the subsurface [65,66]. There are commercial available hybrid AM machining systems that has integrated high speed milling module like LENS 3D Metal

Hybrid by OPTOMEC, Lasertec 65 3D by DMG Mori Seiki, OPM by Sodick, and LUMEX by Matsuura [62].

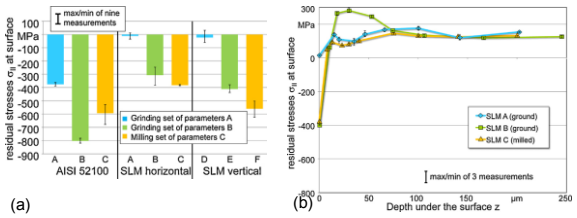

Fig. 5. Effects of post machining on (a) surface residual stress, and (b) residual stress profile of the SLMed component [64].

Brinksmeier et al. [64] characterized the surface integrity of ground and milled SLM samples. Compressive residual stresses were observed in the ground and milled surface as shown in Fig. 5. Oyelola et al. [67] studied the machinability of DED processed Ti6Al4V and observed a 22% increase in compressive residual surface stress of the part because of turning operation from the as-built and heat treatment states. Yamaguchi et al. [68] investigated the surface modification by magnetic field-assisted polishing (MAP) and magnetic field-assisted burnishing (MAB) of 316L stainless steel components made by SLM. Both MAP and MAB can make the residual stress in the surface less tensile. MAB was found to have the capability to convert the tensile residual stress to compressive.

5. Summary and Outlook

This paper gives an overview of the residual stress in metal AM. The residual stress formation mechanism has been proposed and its impact was discussed. The measurement methods of residual stress and its relationship with microstructure were then analysed. The typical residual stress characteristics and its mitigation methods for metal AM were summarized and discussed. Key findings of this work are summarized as follows:

- Residual stress formation in metal AM is mainly caused by high temperature gradient and rapid cooling illustrated by the proposed new model.
- High tensile residual stress is very typical in the surface zone for metal AM while the presence of substrate has a significant influence on residual stress magnitudes.
- Residual stress in metal AM could be mitigated through in-process methods (e.g., preheating, process planning, feedback control, laser peening) and post-process methods (e.g., machining and heat treatment which is the most effective method for relief of residual stress).

Current study on residual stress in AM is in the nascent stage, future research directions remain to be explored include measurement methods for macro/micro residual stresses, crystal structure, simulation, in-process and post-process mitigation, and the impacts on part dimensional accuracy and functionality such as fatigue, creep, and corrosion.

References

[1] Levy GN, Schindel R, Kruth J. Rapid manufacturing and rapid tooling with layer manufacturing (LM) technologies, state of the art and future perspectives. CIRP Ann. Manuf. Technol. 2003;52(2):589-609.
[2] DebRoy T, Wei HL, Zuback JS, Mukherjee T, Elmer JW, Milewski JO, Beese AM, Wilson-Heid A, De A, Zhang W. Additive manufacturing of metallic components – process, structure and properties. Prog Mater Sci 2018; 92:112-224.
[3] Kruth J, Leu M, Nakagawa T. Progress in additive manufacturing and rapid prototyping. CIRP Ann.Manuf. Technol. 1998;47(2):525-540.
[4] Meiners W, Wissenbach K, Gasser A. Shaped body especially prototype or replacement part production, DE Patent 1998;19.
[5] Frazier WE. Metal additive manufacturing: A review. J Mater Eng Perform 2014;23(6):1917-1928.
[6] Murr LE, Gaytan SM, Ramirez DA, Martinez E, Hernandez J, Amato KN, Shindo PW, Medina FR, Wicker RB. Metal fabrication by additive manufacturing using laser and electron beam melting technologies. J. Mater. Sci. & Technol. 2012;28(1):1-14.
[7] Gibson, Rosen, Stucker, Additive manufacturing technologies. Berlin: Springer; 2010.
[8] Flynn JM, Shokrani A, Newman ST, Dhokia V. Hybrid additive and subtractive machine tools – Research and industrial developments. Int. J. Mach. Tools Manuf 2016;10179-101.
[9] Mireles J, Kim H, Lee IH, Espalin D, Medina F, MacDonald E, Wicker R. Development of a fused deposition modeling system for low melting temperature metal alloys. Journal of Electronic Packaging 2013;135(1):011008.
[10] Shiomi M, Osakada K, Nakamura K, Yamashita T, Abe F. Residual stress within metallic model made by selective laser melting process. CIRP Ann. Manuf. Technol. 2004;53(1):195-198.
[11] Mercelis P, Kruth J. Residual stresses in selective laser sintering and selective laser melting. Rapid Prototyping J. 2006;12(5):254-265.
[12] Buchbinder D, Meiners W, Pirch N, Wissenbach K, Schrage J, Investigation on reducing distortion by preheating during manufacture of aluminum components using selective laser melting. J. Laser Appl. 2014;26(1):1-10.
[13] Zaeh MF, Branner G. Investigations on residual stresses and deformations in selective laser melting. Production Engineering 2010;4(1):35-45.
[14] Vilaro T, Colin C, Bartout J. As-fabricated and heat-treated microstructures of the ti-6Al-4V alloy processed by selective laser melting. Metall. Mater. Trans. A 2011;42(10):3190-3199.
[15] Kruth J, Deckers J, Yasa E, WauthléR. Assessing and comparing influencing factors of residual stresses in selective laser melting using a novel analysis method. Proc. Inst. Mech. Eng. Pt. B: J. Eng. Manuf. 2012;226(6):980-991.
[16] Sindo K.. Welding metallurgy. New York: John Wiley & Sons;2003.
[17] Withers P, Bhadeshia H. Residual stress. part 1–measurement techniques. Mater Sci Tech-Lond 2001;17(4):355-365.
[18] Korsunsky AM, Sebastiani M, Bemporad E. Residual stress evaluation at the micrometer scale: Analysis of thin coatings by FIB milling and digital image correlation. Surf Coat Tech 2010:205(7):2393-2403.
[19] Pharr G, Oliver W. Measurement of thin film mechanical properties using nanoindentation. MRS Bull 1992;17(7):28-33.
[20] Tomus D, Tian Y, Rometsch PA, Heilmaier M, Wu X. Influence of post heat treatments on anisotropy of mechanical behaviour and microstructure of hastelloy-X parts produced by selective laser melting. Mat Sci Eng-A 2016;66742-53.
[21] Li C, White R, Fang XY, Weaver M, Guo YB. Microstructure evolution characteristics of Inconel 625 alloy from selective laser melting to heat treatment. Mat Sci Eng-A 2017, 705: 20-31.
[22] Wu AS, D. Brown W, Kumar M, Gallegos GF, King WE. An experimental investigation into additive manufacturing-induced residual stresses in 316L stainless steel. Metall Mater Trans A 2014;1-11.
[23] Amato K, Hernandez J, Murr L, Martinez E, Gaytan S, Shindo P, Collins S. Comparison of microstructures and properties for a ni-base superalloy (alloy 625) fabricated by electron beam melting. J Mater Sci Res 2012;1(2):3.
[24] Vrancken B, Thijs L, Kruth J, Van Humbeeck J. Heat treatment of Ti6Al4V produced by selective laser melting: Microstructure and mechanical properties. J. Alloys Compounds 2012;541(0):177-185.

[25] Wang Z, Palmer TA, Beese AM. Effect of processing parameters on microstructure and tensile properties of austenitic stainless steel 304L made by directed energy deposition additive manufacturing. Acta Materialia 2016;110226-235.
[26] Wang Z, Denlinger E, Michaleris P, Stoica AD, Ma D, Beese AM. Residual stress mapping in inconel 625 fabricated through additive manufacturing: Method for neutron diffraction measurements to validate thermomechanical model predictions. Mater Des 2017;113169-177.
[27] Kruth J, Froyen L, Van Vaerenbergh J, Mercelis P, Rombouts M, Lauwers B. Selective laser melting of iron-based powder. J. Mater. Process. Technol. 2004;149(1):616-622.
[28] Lu Y, Wu S, Gan Y, Huang T, Yang C, Junjie L, Lin J. Study on the microstructure, mechanical property and residual stress of SLM inconel-718 alloy manufactured by differing island scanning strategy. Opt Laser Technol 2015;75197-206.
[29] Li C, Liu Z, Fang X, Guo Y. On the simulation scalability of predicting residual stress and distortion in selective laser melting. J. Manuf. Sci. Eng. 2018, in press doi:10.1115/1.4038893.
[30] Moat R, Pinkerton A, Li L, Withers P, Preuss M. Residual stresses in laser direct metal deposited Waspaloy. Mat Sci Eng-A 2011;528(6):2288-2298.
[31] Yadroitsev I, Yadroitsava I. Evaluation of residual stress in stainless steel 316L and Ti6Al4V samples produced by selective laser melting. Virtual Phys. Prototyping 2015;10(2):67-76.
[32] Bagg SD, Sochalski-Kolbus LM, Bunn JR. The effect of laser scan strategy on distortion and residual stresses of arches made with selective laser melting. 2016;NASA report M16-5377.
[33] Mishurova T, Cabeza S, Artzt K, Haubrich J, Klaus M, Genzel C, Requena G, Bruno G. An assessment of subsurface residual stress analysis in SLM ti-6Al-4V. Materials 2017;10(4):348.
[34] Zhao X, Li S, Zhang M, Liu Y, Sercombe TB, Wang S, Hao Y, Yang R, Murr LE. Comparison of the microstructures and mechanical properties of Ti–6Al–4V fabricated by selective laser melting and electron beam melting. Mater Des 2016;9521-31.
[35] Li C, Guo YB, Zhao JB. Interfacial phenomena and characteristics between the deposited material and substrate in selective laser melting inconel 625. J. Mater. Process. Technol. 2017;243269-281.
[36] Sochalski-Kolbus L, Payzant EA, Cornwell PA, Watkins TR, Babu SS, Dehoff RR, Lorenz M, Ovchinnikova O, Duty C. Comparison of residual stresses in inconel 718 simple parts made by electron beam melting and direct laser metal sintering. Metall Mater Trans A 2015; 46(3):1419-1432.
[37] De Oliveira U, Ocelík V, Hosson JTMD. Residual stress analysis in co-based laser clad layers by laboratory X-rays and synchrotron diffraction techniques, Surf Coat Tech 2006;201(3-4):533-542.
[38] Rangaswamy P, Griffith M, Prime M, Holden T, Rogge R, Edwards J, Sebring R. Residual stresses in LENS® components using neutron diffraction and contour method. Mat Sci Eng-A 2005;399(1-2):72-83.
[39] Denlinger ER., Heigel JC, Michaleris P, Palmer TA. Effect of inter-layer dwell time on distortion and residual stress in additive manufacturing of titanium and nickel alloys. J. Mater. Process. Technol. 2015;215(0):123-131.
[40] Denlinger ER., Heigel JC, Michaleris P. Residual stress and distortion modeling of electron beam direct manufacturing ti-6Al-4V. Proc. Inst. Mech. Eng. Pt. B: J. Eng. Manuf. 2014;0954405414539494.
[41] Szost BA, Terzi S, Martina F, Boisselier D, Prytuliak A, Pirling T, Hofmann M, Jarvis DJ. A comparative study of additive manufacturing techniques: Residual stress and microstructural analysis of CLAD and WAAM printed Ti–6Al–4V components. Mater Des 2016;89559-567.
[42] Mercelis P, Kruth JP. Residual stresses in selective laser sintering and selective laser melting. Rapid Prototyping J 2006 12(5):254-265.
[43] Papadakis L, Loizou A, Risse J, Schrage J. Numerical computation of component shape distortion manufactured by selective laser melting. Procedia CIRP 2014;18(0):90-95.
[44] Keller N, Ploshikhin V. New method for fast predictions of residual stress and distortion of AM parts. 2014;1229-1237.
[45] Li C, Liu JF, Fang XY, Guo YB. Efficient predictive model of part distortion and residual stress in selective laser melting. Addi Manuf 2017;17:157-168.
[46] Desmaison O, Pires P, Levesque G, Peralta A, Sundarraj S, Makinde A, Jagdale V, Megahed M. Influence of computational grid and deposit volume on residual stress and distortion prediction accuracy for additive manufacturing modeling. ICME 2017. Switzerland: Springer International Publishing; 2017.p.365-374.
[47] Berumen S, Bechmann F, Lindner S, Kruth J, Craeghs T. Quality control of laser-and powder bed-based additive manufacturing (AM) technologies. Physics Procedia 2010;5617-622.
[48] Krauss H, Eschey C, Zaeh M. Thermography for monitoring the selective laser melting process, In SFF Symposium, pp. 999-1014. 2012.
[49] G. Tapia, A. Elwany, A review on process monitoring and control in metal-based additive manufacturing,. J Manuf Sci Eng 2014; 136(6): 060801.
[50] Tammas-Williams S, Zhao H, Léonard F, Derguti F, Todd I. Prangnell P., XCT analysis of the influence of melt strategies on defect population in Ti–6Al–4V components manufactured by selective electron beam melting. Mater Charact 2015;10247-61.
[51] Everton SK, Hirsch M, Stravroulakis P, Leach RK, Clare AT. Review of in-situ process monitoring and in-situ metrology for metal additive manufacturing. Mater Design 2016;95(Supplement C):431-445.
[52] Kempen K, Vrancken B, Buls S, Thijs L, Van Humbeeck J, Kruth J. Selective laser melting of crack-free high density M2 high speed steel parts by baseplate preheating. J Manuf Sci Eng 2014;136(6):061026.
[53] Li W, Liu J, Zhou Y, Wen S, et. al. Effect of substrate preheating on the texture, phase and nanohardness of a Ti–45Al–2Cr–5Nb alloy processed by selective laser melting. Scr. Mater. 2016;11813-18.
[54] Vrancken B, Buls S, Kruth J, Van Humbeeck J. Influence of preheating and oxygen content on selective laser melting of Ti6Al4V. Proceedings of the 16th RAPDASA Conference 2015.
[55] Mertens R, Vrancken B, Holmstock N, Kinds Y, Kruth J, Van Humbeeck J. Influence of powder bed preheating on microstructure and mechanical properties of H13 tool steel SLM parts. Physics Procedia 2016; 83882-890.
[56] Ali H, Ma L, Ghadbeigi H, Mumtaz K. In-situ residual stress reduction, martensitic decomposition and mechanical properties enhancement through high temperature powder bed pre-heating of selective laser melted Ti6Al4V. Mat Sci Eng-A 2017;695211-220.
[57] Sealy M, Madireddy G, Li C, Guo Y. Finite element modeling of hybrid additive manufacturing by laser shock peening. The 27th Annual International Solid Freeform Fabrication Symposium 2016;306-316.
[58] Kalentics N, Boillat E, Peyre P, Ćirić-Kostić S, Bogojević N, LogévRE. Tailoring residual stress profile of selective laser melted parts by laser shock peening. Addi Manuf 2017; 1690-97.
[59] Gu J, Wang X, Bai J, Ding J, Williams S, Zhai Y, Liu K. Deformation microstructures and strengthening mechanisms for the wire arc additively manufactured al-Mg4. 5Mn alloy with inter-layer rolling, Mat Sci Eng-A 2018;712292-301.
[60] Sealy MP, Madireddy G, Williams R., Rao P, Toursangsaraki M. Hybrid processes in additive manufacturing. J. Manuf. Sci. Eng. 2018, in press doi:10.1115/1.4038644.
[61] Kreitcberg A, Brailovski V, Turenne S. Effect of heat treatment and hot isostatic pressing on the microstructure and mechanical properties of inconel 625 alloy processed by laser powder bed fusion. Mat Sci Eng-A 2017;6891-10.
[62] König W, Berktold A, Koch K. Turning versus grinding–a comparison of surface integrity aspects and attainable accuracies. CIRP Ann-Manuf Techn 1993;42(1):39-43.
[63] Matsumoto Y, Hashimoto F, Lahoti G. Surface integrity generated by precision hard turning, CIRP Ann-Manuf Techn 1999;48(1):59-62.
[64] Brinksmeier E, Levy G, Meyer D, Spierings A. Surface integrity of selective-laser-melted components, CIRP Ann-Manuf Techn 2010; 59(1): 601-606.
[65] Oyelola O, Crawforth P, M'Saoubi R, Clare AT. On the machinability of directed energy deposited Ti6Al4V. Addi Manuf 2018;1939-50.
[66] Yamaguchi H, Fergani O, Wu P. Modification using magnetic field-assisted finishing of the surface roughness and residual stress of additively manufactured components. CIRP Ann-Manuf Techn 2017; 66(1):305-308.